Reduced order models for parameterized hyperbolic conservations laws with shock reconstruction

By P. G. Constantine AND G. Iaccarino

1. Introduction

Continued advances in high performance computing are enabling researchers in computational science to simulate more complex physical models. Such simulations can occupy massive supercomputers for extended periods of time. Unfortunately, the cost of these complex simulations renders parameter studies (e.g., design optimization or uncertainty quantification) infeasible, where multiple simulations must be run to explore the space of design parameters or uncertain inputs. A common fix is to construct a cheaper surrogate model – trained on a few carefully selected simulation runs – for use in the parameter study.

Model reduction for large-scale simulations is an active research field. Techniques such as reduced basis methods (Prud'homme *et al.* 2002; Veroy & Patera 2005) and approaches based the proper orthogonal decomposition (Willcox & Peraire 2002; Rowley *et al.* 2004) have been used to successfully build cheaper surrogate models for certain problems; the cost reduction has been dramatic in many cases. In the statistical literature, various methods exist for constructing Gaussian process approximations to physical systems (Higdon *et al.* 2008) with a comparable goal of cost reduction for parameter studies. Similarly, methods based on global polynomial approximation are often used in uncertainty quantification for statistical inverse problems (Marzouk *et al.* 2007) or to approximate integrated statistics of model outputs (Xiu & Karniadakis 2002).

All such methods perform well when the solution of the physical model is smooth with respect to variations in the inputs, such as parabolic and elliptic partial differential equation models that depend continuously on a set of input parameters. However, when the solution contains a discontinuity – or even a sharp gradient – with respect to the parameter, many of these methods smooth out important sharp features at best or exhibit oscillations near sharp features (e.g., Gibbs phenomena) at worst. It has been observed that solutions that contain sharp gradients and discontinuities in physical space – such as the solution of a hyperbolic conservation law – often contain comparable discontinuities in parameter space. Thus, accurate surrogate construction for parameterized conservation laws has proved challenging for methods based on interpolation, Galerkin projection, or least-squares approximation such as those mentioned above.

There have been numerous attempts to adjust approximation models to accurately capture sharp, local features in parameter space (Millman *et al.* 2006; Archibald *et al.* 2009; Jakeman *et al.* 2011), including many inspired by methods for approximating the discontinuous solutions of hyperbolic conservation laws (Abgrall 2008; Barth 2011; Haasdonk & Ohlberger 2008; Witteveen & Iaccarino 2012). These methods ultimately need to resolve the local features with sufficiently high resolution in the parameter domain, which do not scale well to problems with many input parameters, where the discontinuity

itself may be a hypersurface in a high dimensional space. Another class of methods uses global parameter approximations (e.g., polynomials) with a Galerkin projection (Poette *et al.* 2009; Pettersson *et al.* 2010; Tryoen *et al.* 2010, 2012) in the parameter space. But such approaches rarely produce pointwise accurate approximations even with many basis elements.

In this work, we present an alternative approach for constructing a reduced order model of a solution of a hyperbolic conservation law with discontinuities or sharp gradients. Assume that we have computed and stored the time histories of solutions for a handful of chosen points in the input parameter space. The goal is to use these stored solutions to approximate the solution at some other point in the input parameter space without rerunning the full simulation. It has been observed that the solution depends smoothly on the input parameters in most of the physical domain, while physical regions that contain discontinuities are relatively small. We wish to take advantage of this when constructing the reduced order model.

We first approximate the solution using a standard surrogate approach – such as a low order global polynomial. We then use the gradient of this approximation with respect to the parameters to define regions in the physical space where the discontinuity is likely to occur. Given these regions, we return to the physical model (i.e., the conservation law) and correct the regions where the reduced order model is likely to be inaccurate. In other words, we solve the conservation law on a set of smaller domains indicated by the gradient of the surrogate with respect to the parameters; the boundary and initial conditions are set by the smooth parameter approximation. Separated regions can be computed independently in parallel.

This idea is remarkable for its conceptual simplicity; it leverages the strengths of both smooth interpolation methods and established techniques for capturing the discontinuities arising in the solution of hyperbolic conservation laws. Its disadvantage is that it is *intrusive* in the following sense: one may not simply rerun the existing simulation code at different points in the parameter space to construct the approximation. Instead, one needs a solver for the conservation law that takes arbitrary initial conditions and time-dependent boundary conditions that can function on subregions of the physical domain.

The remainder of the paper proceeds as follows. In Section 2, we formally describe the approximation procedure, including heuristics for determining the regions for reconstruction. To keep the notation manageable and the discussion concise we describe the conservation law and the model reduction method in one spatial dimension. However, the idea easily extends to higher spatial dimensions. In Section 3, we apply the method to the inviscid Euler equations for compressible flow in one spatial dimension with one parameter describing the initial condition. Section 4 concludes with a discussion and directions for further research.

2. A surrogate model with shock reconstruction

Let $u = u(x, t, s) \in \mathbb{R}^M$ represent the conserved variables in a system of M conservation laws; the quantities u depend on a spatial coordinate $x \in \mathcal{X} \subset \mathbb{R}$, a temporal coordinate $t \in [0, T]$, and parameters $s \in \mathcal{S} \subset \mathbb{R}^d$. Let u satisfy the conservation law

$$\frac{\partial}{\partial t} u + \frac{\partial}{\partial x} f(u, s) = 0 \tag{2.1}$$

where $f = f(u, s)$ is the nonlinear flux function subject to the given boundary and initial conditions

$$\begin{array}{rcll} Au & = & b(x,t,s), & x \in \partial\mathcal{X}, \quad t \in [0,T] \\ u & = & c(x,s), & x \in \mathcal{X}, \quad t = 0, \end{array} \tag{2.2}$$

where the $M \times M$ matrix A ensures the problem is well-posed with regards to the incoming and outgoing characteristics. Note that the input parameters s may effect the flux function, the initial conditions, and/or the boundary conditions; we assume that the problem is well-posed for all input parameters $s \in \mathcal{S}$. It is well known that the solution u may develop discontinuities in space with smooth initial and boundary data. We make the following assumption about the influence of the parameters on the solution u.

ASSUMPTION 1. *Let $x^* = x^*(t,s) \in \mathcal{X}$ be a point in space at a fixed time t where the solution u is discontinuous in space. We assume that x^* depends nontrivially on the input parameters s.*

If the location of the discontinuity does not depend on the parameter, then one can split the parameter domain $\mathcal{S}$ according to the locations of the discontinuities and construct smooth parameter approximations on each subdomain. However, this situation rarely occurs in practice. Typically, one is interested in the change in the location of the discontinuity – judged by the results of numerical simulations – as the parameters vary. Thus, we restrict ourselves to the case where the position of the discontinuity depends nontrivially on the parameter value.

Assumption 1 implies that the solution u is discontinuous with respect to parameter variation as well as spatial variation. To see this, let u^+ and u^- be the values of the solution on either side of the discontinuity at x^*, where the "+" and "−" are related to the direction normal to the discontinuity surface. If x^* changes as the parameter changes from s to $s + \Delta s$, then there will be a region in $\mathcal{X}$ where $u = u^-$ for parameter s but $u = u^+$ for parameter $s + \Delta s$; see Figure 1. This discontinuity in the parameter space degrades the performance of global approximations in parameter space, such as polynomial-based methods and Gaussian process methods.

The solution u is typically smooth away from regions containing discontinuities both in physical and parameter space. The relatively small and isolated regions containing discontinuities preclude the use of global parameter approximations. For a fixed parameter value where we wish to approximate u, we propose a method to detect troublesome regions in physical space and apply a relatively cheap local correction that reconstructs the discontinuities.

2.1. *A global surrogate*

Let $s_k \in \mathcal{S}$ be a set of design points in the parameter space with $k = 1, \ldots, p$. For each s_k, a high fidelity solver computes the solution to the conservation law (2.1) at a chosen spatial discretization denoted x_i, $i = 1, \ldots, m$ and temporal discretization denoted t_j, $j = 1, \ldots, n$. Let $u_k = u(x_i, t_j, s_k)$ be the solution with inputs s_k at the point x_i and time t_j. For notational convenience, we assume that the solutions to the parameterized conservation law exist on the same spatiotemporal discretization; this assumption can be relaxed. Let $q = q(u(x,t,s)) \in \mathbb{R}$ be a time/space/parameter dependent scalar quantity of interest computed from the conserved variables. We choose q so that it exhibits the same shocks and discontinuities as the conserved variables; for example, in the Euler equations in Section 4, q will be pressure. Let $q_k = q(u_k)$.

To approximate the solution and quantity of interest at some other point s in the input

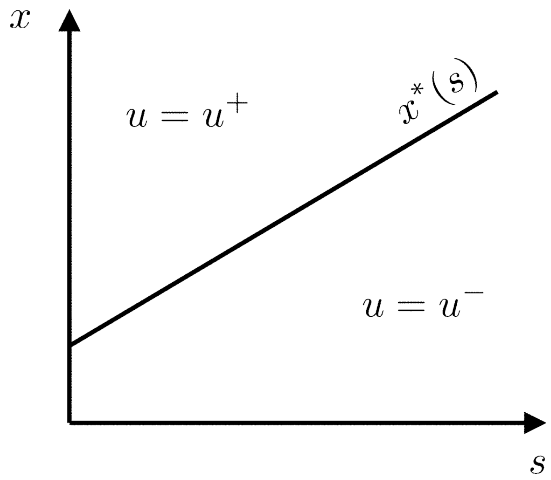

FIGURE 1. Representation at a fixed time t of a shock location $x^*(t,s)$ in the solution $u = u(x,t,s)$ of a hyperbolic conservation law that depends on an input parameter. For a fixed parameter value s, the solution u contains a discontinuity as a function of x. Similarly, for a fixed x, the solution u contains a discontinuity as a function of s.

parameter space $\mathcal{S}$, we compute the interpolant

$$\begin{array}{rcccl} u(x_i,t_j,s) & \approx & \tilde{u}(x_i,t_j) & = & \mathcal{I}_s(s;\, u_1,\ldots,u_p), \\ q(x_i,t_j,s) & \approx & \tilde{q}(x_i,t_j) & = & \mathcal{I}_s(s;\, q_1,\ldots,q_p), \end{array} \tag{2.3}$$

where $\mathcal{I}_s$ is an interpolation operator in the parameter space. Possible interpolation methods include splines, polynomials, or Gaussian process approximations.

2.2. *Regions with sharp parameter gradients*

The parameter interpolation occurs independently at each time t_j and each point in space x_i. We expect the approximation $\tilde{q}$ to be poor at locations x_i where basis elements $\{q_k\}$ fall on either side of a discontinuity. Therefore, we compute the gradient of the parameter interpolant $\tilde{q}$ with respect to the parameters at each point in the space/time discretization (x_i,t_j) and check its magnitude.

Define the partial derivatives of $\tilde{q}$ by

$$\frac{\partial \tilde{q}}{\partial s_\ell}(x_i,t_j) \;=\; \frac{\partial}{\partial s_\ell}\mathcal{I}_s(s;\, q_1,\ldots,q_p), \qquad \ell = 1,\ldots,d. \tag{2.4}$$

This gradient is easily computed in the case of common interpolation schemes such as polynomial interpolation or Gaussian process approximation. Define the Jacobian

$$J \;=\; J(x_i,t_j) \;=\; \left[\begin{array}{ccc} \frac{\partial \tilde{q}}{\partial s_1} & \cdots & \frac{\partial \tilde{q}}{\partial s_d} \end{array}\right]. \tag{2.5}$$

For a specified threshold ε, if $\|J\|_\infty > \varepsilon$, then (x_i,t_j) is tagged as a point requiring a correction. (We will discuss the choice of the threshold ε in the numerical examples in Section 3.)

By checking if $\|J\|_\infty > \varepsilon$ over the space/time discretization, we obtain spatial regions where we trust the parameter interpolants $\tilde{q}$ and $\tilde{u}$ and regions where they need to be corrected; we next discuss the correction procedure.

2.3. *Discontinuity reconstruction*

To construct the reduced order model, we solve the original conservation law (2.1) on a domain that contains the regions needing correction and modify the parameter interpolant. By this approach, we can use tested numerical techniques for capturing spatial discontinuities in conservation laws (Leveque 2002), and we need not seek special parameter approximations that resolve sharp features. The initial and boundary conditions for the problem defining the correction come from the parameter interpolant $\tilde{u}$, which we consider trustworthy in regions with $\|J\|_\infty < \varepsilon$.

Define the set of spatial points

$$Y_{t_j} \;=\; \{(x_i, t_j) \;:\; \|J\|_\infty > \varepsilon\}, \qquad \bar{Y}_{t_j} \;=\; \{(x_i, t_j) \;:\; \|J\|_\infty \leq \varepsilon\} \tag{2.6}$$

and note the dependence of these sets on the time point t_j. Let τ be the smallest t_j for which Y_{t_j} is non-empty, i.e., the first point in time where we wish to correct the approximation. Define the continuous spatial region $\mathcal{Y}_\tau \subset \mathcal{X}$ as a spatial subset of the physical domain that contains the points Y_τ. The region $\mathcal{Y}_\tau$ will be the spatial domain for the problem defining the correction. For now, assume there is only one connected spatial region in $\mathcal{Y}_\tau$.

Formally, we set the initial condition by spatially interpolating $\tilde{u}$ over $\mathcal{Y}_\tau$ at time $\tau - \Delta t$. We trust the spatial interpolation since $\|J\|_\infty < \varepsilon$ for all spatial points at time $\tau - \Delta t$. For $x \in \mathcal{Y}_\tau$, let

$$c_{\mathcal{Y}}(x) \;=\; \mathcal{I}_x\big(x;\, \tilde{u}(x_1, \tau - \Delta t), \ldots, \tilde{u}(x_m, \tau - \Delta t)\big) \tag{2.7}$$

be the initial condition for the correction, where $\mathcal{I}_x$ is a spatial interpolation operator.

For the time-dependent boundary conditions, we first use the spatial interpolation operator to construct the solution on the boundary $\partial\mathcal{Y}_\tau$ at time $\tau - \Delta t$,

$$b_{\mathcal{Y}}^{(\tau-\Delta t)}(x) = \mathcal{I}_x\big(x;\, \tilde{u}(x_1, \tau - \Delta t), \ldots, \tilde{u}(x_m, \tau - \Delta t)\big). \tag{2.8}$$

For the boundary at time τ, we can use only the points from $\bar{Y}_\tau$, since they are trusted,

$$b_{\mathcal{Y}}^{(\tau)}(x) = \mathcal{I}_x\big(x;\, \{\tilde{u}(x_i, \tau) \;:\; (x_i, \tau) \in \bar{Y}_\tau\}\big). \tag{2.9}$$

If $\partial\mathcal{Y}_\tau$ coincides with the original boundary $\partial\mathcal{X}$, then we use the original boundary conditions b from (2.2). We then define the boundary condition on $\mathcal{Y}_\tau$ as a linear temporal interpolation,

$$b_{\mathcal{Y}}(x,t) \;=\; \beta\, t + b_{\mathcal{Y}}^{(\tau-\Delta t)}(x), \qquad \beta = \beta(x) = \frac{b_{\mathcal{Y}}^{(\tau)}(x) - b_{\mathcal{Y}}^{(\tau-\Delta t)}(x)}{\Delta t}. \tag{2.10}$$

If the time step is sufficiently small, then this linear approximation will be adequate. This can be improved with higher order temporal interpolation by using $\tilde{u}$ at more times in the past.

With the interpolated boundary and initial conditions, we compute the solution $v = v(x,t)$ defined on $\mathcal{Y}_\tau \times [\tau - \Delta t, \tau]$ using the conservation law

$$\frac{\partial}{\partial t}\, v + \frac{\partial}{\partial x}\, f(v, s) = 0 \tag{2.11}$$

subject to

$$\begin{array}{rcll} Av & = & b_{\mathcal{Y}}(x,t), & x \in \partial\mathcal{Y}_\tau, \quad t \in [\tau - \Delta t, \tau], \\ v & = & c_{\mathcal{Y}}(x), & x \in \mathcal{Y}_\tau, \quad t = \tau - \Delta t. \end{array} \tag{2.12}$$

The computed solution v serves as the correction term for the approximation $\tilde{u}$ in the

region $\mathcal{Y}_\tau$. Since v is itself the solution to a conservation law, it may also exhibit discontinuities in space.

To apply the correction at time τ, we formally define the corrected approximation (i.e., the reduced order model) $\bar{u}$ as

$$u(x_i,\tau) \approx \bar{u}(x_i,\tau) = \begin{cases} v(x_i,\tau), & x_i \in \mathcal{Y}_\tau, \quad \text{(parameter interpolant)} \\ \tilde{u}(x_i,\tau), & x_i \in \mathcal{X}\backslash\mathcal{Y}_\tau, \quad \text{(computed correction).} \end{cases} \tag{2.13}$$

Given the reduced order model $\bar{u}$ defined at time τ over all spatial nodes $x_1,\ldots,x_m$, we repeat the process to move from time τ to time $\tau+\Delta t$, which involves the construction of the domain $\mathcal{Y}_{\tau+\Delta t}$ from the points $Y_{\tau+\Delta t}$ (see (2.6)) and a similar treatment of the boundary and initial conditions. We continue this iteration up to the final time T. Note that if at any point in time the point sets Y_{t_j} define disconnected regions in space, these regions can be treated independently and in parallel.

3. Numerical Examples

We demonstrate our approach on the Euler equations for compressible flow in one space dimension. For conserved variables density ρ, momentum ρu, and energy E, the nonlinear conservation law is

$$\frac{\partial}{\partial t}\begin{bmatrix}\rho\\ \rho u\\ E\end{bmatrix} + \frac{\partial}{\partial x}\begin{bmatrix}\rho u\\ \rho u^2+p\\ (E+p)u\end{bmatrix} = 0, \quad x\in[-1.5,1.5], \quad t\in[0,3], \tag{3.1}$$

where p is pressure. The closure equation for an ideal polytropic gas is

$$E = \frac{p}{\gamma-1} + \frac{1}{2}\rho u^2, \tag{3.2}$$

where we choose $\gamma = 1.4$ corresponding to air. The scalar quantity of interest we choose is the pressure p, which we will use for defining the untrusted regions. It is well known that the nonlinearity in the flux function results in discontinuities in the conserved variables and pressure, even for smooth initial data. The test problem we will use can be found in Leveque (2002) with associated software available at `www.clawpack.org`.

The high fidelity solution is computed with a finite volume method using a Roe method for an approximate Riemann solver as described in Leveque (2002). The grid has 501 cells, and the time step is $\Delta t = 0.002$. All computations were performed with Matlab R2012a on a 2009 MacBook Pro.

3.1. *Initial and boundary conditions*

We consider a gas initially at rest ($\rho u = 0$) with a bump in the initial density and energy. The height of the bump is parameterized by $s\in[0,20]$. The initial conditions are given by the equations

$$\rho(x,t=0,s) = 1 + s\exp\left(-80x^2\right), \quad \rho u(x,t=0,s) = 0, \quad E(x,t=0,s) = \frac{\rho}{\gamma}. \tag{3.3}$$

The parameter s affects how quickly the waves in density and energy will propagate toward the boundary. Thus, this system satisfies Assumption 1 – that parameter variations affect the spatial locations of the discontinuities that develop.

The right boundary condition is a simple extrapolation from within the domain representing outflow of the characteristics. The left boundary condition is a solid wall that

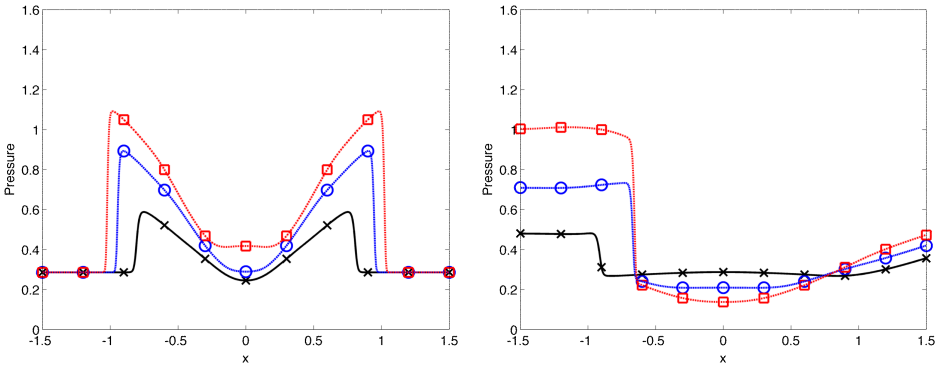

(a) $t = 0.8$ (b) $t = 2.4$

FIGURE 2. Pressure at times $t = 0.8$ before the reflection at the left and $t = 2.4$ after the reflection for parameter values $s = 4$ (x), 12 (circle), and 20 (box). The parameter controls the height of the bump in the initial density. The locations of the shocks subsequently depend on the parameter value.

reflects outgoing characteristics. The spatial distribution of density p at times $t = 0.8$ (before the reflection) and $t = 2.4$ (after the reflection) are shown in Figure 3.1 for three different initial bump heights: $s = 4$, 12, and 20.

3.2. *Global approximations*

We compare four approaches for computing the parameter interpolant: (i) a quadratic polynomial, (ii) a degree 32 polynomial, (iii) a Gaussian process approximation with unknown quadratic mean, and (iv) a least-squares approximation to mimic the behavior of projection-based model reduction methods. Ultimately, we will use the quadratic polynomial as the initial approximation for the reduced order model. However, we will showcase the behavior of the other techniques in what follows to demonstrate the need for the correction.

All parameter approximations are linear combinations of solutions computed at selected points s_k in the input parameter space. The specific points s_k and the coefficients of the linear approximation depend on the approximation technique. We test the schemes' ability to approximate the solution at some input parameter s not in the training set $\{s_k\}$. For each method, the approximation of the pressure near the left shock before reflection is compared to the true pressure at parameter $s = 13.2$ and time $t = 1$ are plotted in Figure 3.2.

(LOP) A low-order (quadratic) polynomial approximation has the advantage of using only three points in the parameter domain to construct the approximation. However, it is very limited in its ability to reproduce sharp, local features. We will see that approximations of the discontinuity in physical space exhibit a characteristic stair step behavior that results from using three solutions with shocks in different locations. This behavior has been observed in Poette *et al.* (2009). The points we choose correspond to the two endpoints and the midpoint of the interval. Note that this is equivalent to the points in a three-point Clenshaw-Curtis integration rule. (Figure 3(a).)

(HOP) With a high-order polynomial approximation (degree 32), we expect very accurate approximation in smooth regions of the solution. However, near the discontinuity in parameter space, the approximation exhibits the well-known Gibbs phenomena. This reveals itself in the physical domain as oscillations near the discontinuity in space. Note

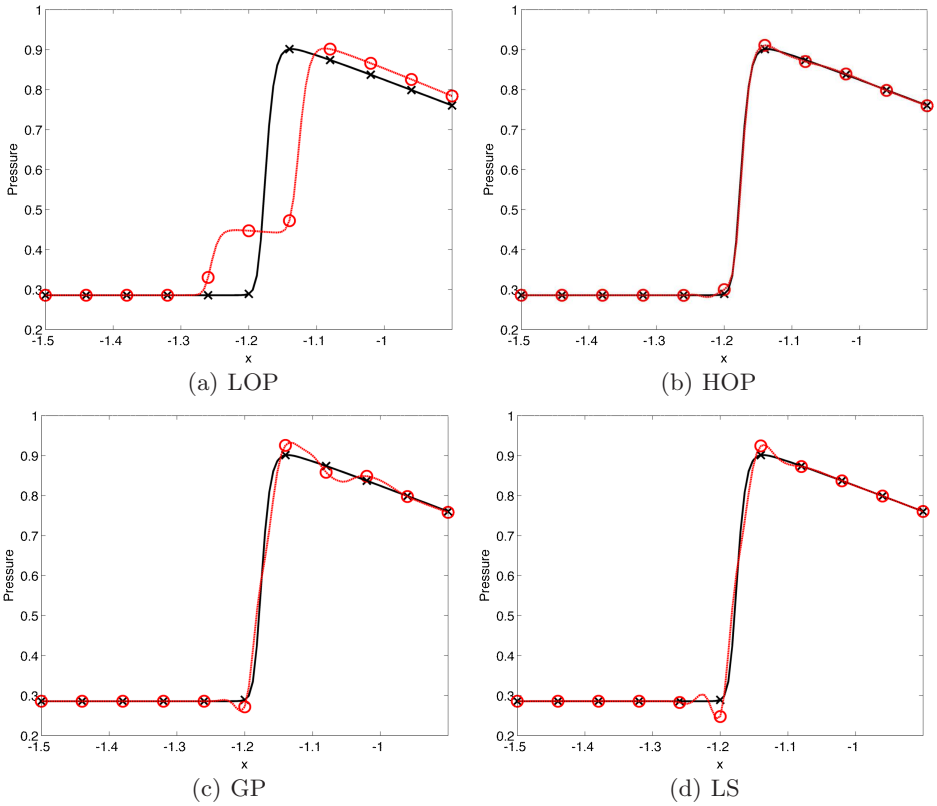

FIGURE 3. Examining the approximation properties of various parameter interpolation schemes: a quadratic polynomial (Figure 3(a)), a degree 32 polynomial (Figure 3(b)), a Gaussian process approximation (Figure 3(c)), and a least-squares approximation (Figure 3(d)). In each figure, the symbol x is the true solution and the circle is the approximation. The figures zoom in on the shock in the density at the left side of the physical domain at time $t = 1$ to display each method's ability to recreate the physical discontinuity.

that refining the approximation in space does not reduce this phenomena. We construct the degree 32 polynomial by interpolating the solution computed at the points of a 33-point Clenshaw-Curtis integration rule. (Figure 3(b).)

(GP) Gaussian process approximation methods have become popular for accurate interpolation of scattered, high dimensional data. We apply an approximation with an unknown quadratic mean using eleven uniformly spaced points in the parameter space and correlation length parameter $\alpha = 3.33$. (Figure 3(c).)

(LS) Reduced basis methods with Galerkin projection minimize the energy norm of the error. However, the least-squares solution and the minimum energy norm solution are comparable. Instead of specifically implementing all varieties of reduced basis methods on the nonlinear Euler equations, we compute the coefficients of a least-squares approximation over the discrete physical domain. In practice, this is not possible since the least-squares approximation requires the true solution to compute the coefficients. For our purpose of comparing approximation methods, this approach suffices, and we compute a least-squares projection over the spatial domain for each time t_j. In this example, the s_k are eleven uniformly distributed points over the parameter domain. (Figure 3(d).)

3.3. *Computing the correction to reconstruct the shock*

In principle, we could use any of the above approximations as the global approximation $\tilde{u}$ of the conserved variables. However, in practice we expect our flow simulations to be expensive, and we wish to use the parameter approximation with the fewest points in the parameter space. For this reason, we employ the quadratic polynomial as the initial approximation for the reduced order model. Additionally, oscillations in the function imply oscillations in the spatial derivative, which causes problems for the derivative-based heuristic for marking untrusted regions. So we prefer underresolved approximations for those reasons. We should use an approximation whose parameter gradient (see (2.4)) is easy to compute. Of the four approximations above, the polynomial and Gaussian process approximations admit this feature. The parameter gradient of the least-squares approximation requires the derivative of the true pressure with respect to the parameters; this is generally out of reach for most problems.

Figure 4(a) displays a histogram of the derivative of pressure approximations with respect to the parameter s at each point in space and time. We can use this to get an idea of the tolerance to set for marking untrusted regions. Figure 4(b) plots the gradient over space time, where we note that large gradient values appear to follow the shocks nicely. Figures 4(c) and 4(d) show the marked space/time regions in red for tolerances 0.1 and 0.01, respectively.

We solve the Euler equations on the subdomains requiring correction, where we use the trusted values of the parameter interpolant to set boundary and initial conditions. The equations are solved with a finite volume scheme using a Roe method for the approximate Riemann solver as detailed in Leveque (2002). We use a finer spatial grid and smaller time step to compute the fixed regions. Currently, this approach increases the cost of the reconstruction considerably. We plan to optimize such computations in future work.

Figure 3.3 compares the original low-order polynomial approximation with the corrected approximation – both against the true solution at the parameter $s = 13.2$ for times $t = 0.6$, 1.2, 1.8, and 2.4. The dark circles at the bottom of the plot indicate the regions where the fix is being applied; this corresponds to a tolerance of 0.05.

We have avoided a direct comparison of computational cost, since in the current implementation, the full model takes less time to compute than the reduced model. However, we are optimistic that given the proper computational setting – e.g., a massively parallel machine with sufficient hard disk space – the algorithms can be implemented in such a way so as to achieve considerable savings.

4. Conclusion

We have presented a method for constructing a reduced order model for a parameterized hyperbolic conservation law. Standard model reduction methods perform well for models whose solution depends smoothly on the parameters, but struggle with models whose solutions contains sharp gradients or discontinuities. The proposed method uses a standard method as an initial guess to approximate the solution at a new point in the parameter space. It then uses the space/time varying parameter gradient to mark regions where the approximation is likely to be poor. It then returns to the conservation law to correct the marked regions.

The goal of a model reduction method is to approximate the solution with less computational effort than the high fidelity model. While the proposed method nominally contains fewer degrees of freedom in space/time for a fixed parameter value, the implementation

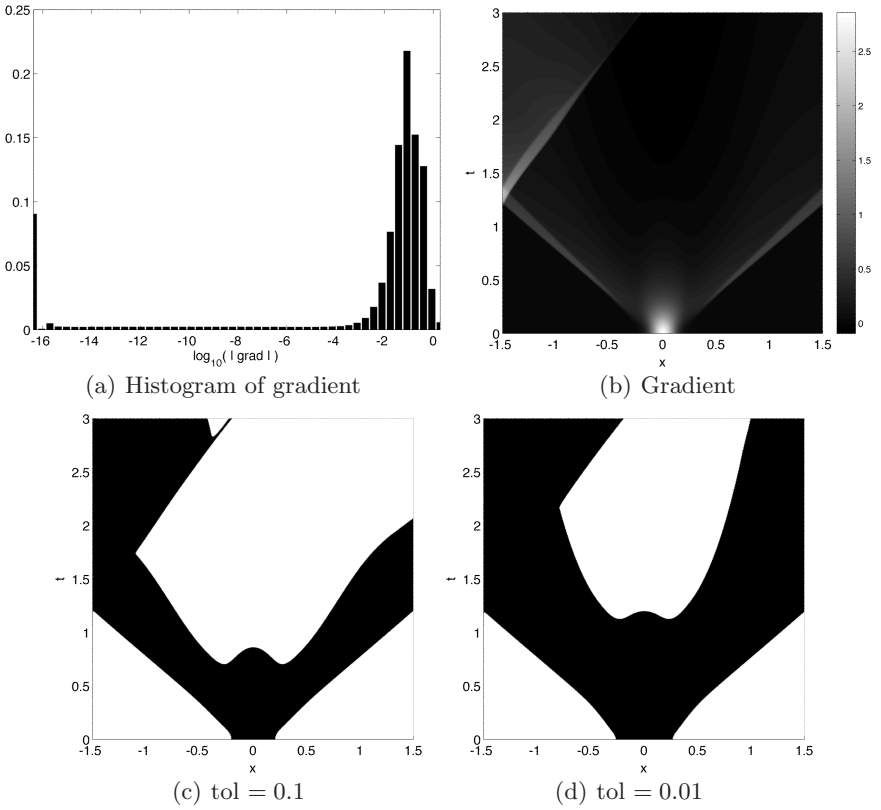

(a) Histogram of gradient (b) Gradient

(c) tol = 0.1 (d) tol = 0.01

FIGURE 4. The gradient of the parameter approximation. Figures 4(c) and 4(d) show the regions in space/time marked for correction for two tolerances; the marked regions are in black and the ignored regions are in white.

is not straightforward. Cost reduction will depend heavily on the data structures and code optimization techniques employed in the computation of the correction. However, we are optimistic that substantial reduction is possible.

Future work will include extension to two spatial dimensions and more parameters. In particular, we are interested in problems where parameters affect the location of localized features in the initial condition. Such problems are very difficult for standard projection-based reduced order models. We expect further improvement in the criteria for marking regions, which may include a contribution from the variance with respect to the parameters or some other measure of error. With that, we expect to gain further insight into selection of the tolerance.

REFERENCES

ABGRALL, R. 2008 A simple, flexible and generic deterministic approach to uncertainty quantifications in non linear problems: application to fluid flow problems .

ARCHIBALD, R., GELB, A., SAXENA, R. & XIU, D. 2009 Discontinuity detection in multivariate space for stochastic simulations. *J. of Comp. Phys.* **228** (7), 2676 – 2689.

BARTH, T. 2011 On the propagation of statistical model parameter uncertainty in cfd calculations. *Theoretical and Computational Fluid Dynamics* pp. 1–23.

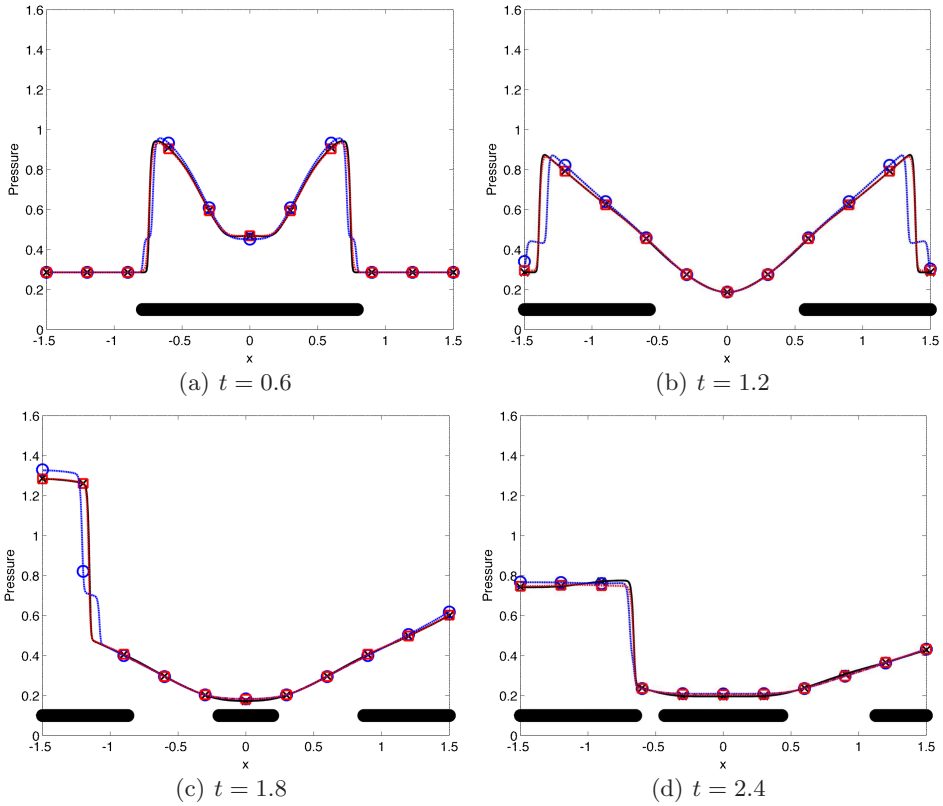

FIGURE 5. A comparison of a low-order polynomial approximation with and without the correction at various times. The symbol x is the truth, the circle is the interpolant without correction, and the square is the interpolant with correction. The black marks at the bottom of each figure identify the regions where the correction is applied for a tolerance of 0.05.

HAASDONK, B. & OHLBERGER, M. 2008 Reduced basis method for explicit finite volume approximations of nonlinear conservation laws. In *Proceedings of the 12th International Conference on Hyperbolic Problems: Theory, Numerics, Application*, p. 605614. AMS, Providence, RI.

HIGDON, D., GATTIKER, J., WILLIAMS, B. & RIGHTLEY, M. 2008 Computer model calibration using high-dimensional output. *J. of the American Statistical Association* **103** (482), 570–583.

JAKEMAN, J. D., ARCHIBALD, R. & XIU, D. 2011 Characterization of discontinuities in high-dimensional stochastic problems on adaptive sparse grids. *J. of Comp. Phys.* **230** (10), 3977 – 3997.

LEVEQUE, R. J. 2002 *Finite Volume Methods for Hyperbolic Problems*. Cambridge University Press.

MARZOUK, Y. M., NAJM, H. N. & RAHN, L. A. 2007 Stochastic spectral methods for efficient Bayesian solution of inverse problems. *J. of Comp. Phys.* **224** (2), 560 – 586.

MILLMAN, D. R., KING, P. I., MAPLE, R. C., BERAN, P. S. & CHILTON, L. K. 2006 Uncertainty Quantification with a B-Spline Stochastic Projection. *AIAA Journal* **44**, 1845–1853.

PETTERSSON, P., NORDSTROM, J. & IACCARINO, G. 2010 Boundary procedures for

the time-dependent burgers' equation under uncertainty. *Acta Mathematica Scientia* **30** (2), 539 – 550.

Poette, G., Despres, B. & Lucor, D. 2009 Uncertainty quantification for systems of conservation laws. *J. of Comp. Phys.* **228** (7), 2443 – 2467.

Prud'homme, C., Rovas, D. V., Veroy, K., Machiels, L., Maday, Y., Patera, A. T. & Turinici, G. 2002 Reliable real-time solution of parametrized partial differential equations: Reduced-basis output bound methods. *J. of Fluids Engineering* **124** (1), 70–80.

Rowley, C. W., Colonius, T. & Murray, R. M. 2004 Model reduction for compressible flows using POD and Galerkin projection. *Physica D: Nonlinear Phenomena* **189** (1-2), 115 – 129.

Tryoen, J., Maitre, O. & Ern, A. 2012 Adaptive anisotropic spectral stochastic methods for uncertain scalar conservation laws. *SIAM J. on Sci. Comp.* **34** (5), A2459–A2481.

Tryoen, J., Maitre, O. L., Ndjinga, M. & Ern, A. 2010 Intrusive Galerkin methods with upwinding for uncertain nonlinear hyperbolic systems. *J. of Comp. Phys.* **229** (18), 6485 – 6511.

Veroy, K. & Patera, A. T. 2005 Certified real-time solution of the parameterized steady incompressible navier-stokes equations: rigorous reduced-basis *a posteriori* error bounds. *Int. J. for Numerical Methods in Fluids* **47**, 77—788.

Willcox, K. & Peraire, J. 2002 Balanced Model Reduction via the Proper Orthogonal Decomposition. *AIAA Journal* **40** (11), 2323–2330.

Witteveen, J. & Iaccarino, G. 2012 Simplex stochastic collocation with random sampling and extrapolation for nonhypercube probability spaces. *SIAM J. on Sci. Comp.* **34** (2), A814–A838.

Xiu, D. & Karniadakis, G. 2002 The Wiener–Askey polynomial chaos for stochastic differential equations. *SIAM J. on Sci. Comp.* **24** (2), 619–644.